A Destabilizing Domain Allows for Fast, Noninvasive, Conditional Control of Protein Abundance in the Mouse Eye – Implications for Ocular Gene Therapy

Shyamtanu Datta,[1] Marian Renwick,[1] Viet Q. Chau,[1] Fang Zhang,[1] Emily R. Nettesheim,[2] Daniel M. Lipinski,[2,3] and John D. Hulleman[1,4]

[1]Department of Ophthalmology, University of Texas Southwestern Medical Center, Dallas, Texas, United States
[2]Department of Ophthalmology, Eye Institute, Medical College of Wisconsin, Milwaukee, Wisconsin, United States
[3]Nuffield Laboratory of Ophthalmology, Department of Clinical Neuroscience, University of Oxford, Oxford, United Kingdom
[4]Department of Pharmacology, University of Texas Southwestern Medical Center, Dallas, Texas, United States

Correspondence: John D. Hulleman, Departments of Ophthalmology and Pharmacology, University of Texas Southwestern Medical Center, 5323 Harry Hines Boulevard, Dallas, TX 75390-9057, USA; John.Hulleman@UTSouthwestern.edu.

Submitted: June 11, 2018
Accepted: August 30, 2018

Citation: Datta S, Renwick M, Chau VQ, et al. A destabilizing domain allows for fast, noninvasive, conditional control of protein abundance in the mouse eye – implications for ocular gene therapy. *Invest Ophthalmol Vis Sci*. 2018;59:4909–4920. https://doi.org/10.1167/iovs.18-24987

Purpose. Temporal and reversible control of protein expression in vivo is a central goal for many gene therapies, especially for strategies involving proteins that are detrimental to physiology if constitutively expressed. Accordingly, we explored whether protein abundance in the mouse retina could be effectively controlled using a destabilizing *Escherichia coli* dihydrofolate reductase (DHFR) domain whose stability is dependent on the small molecule, trimethoprim (TMP).

Methods. We intravitreally injected wild-type C57BL6/J mice with an adeno-associated vector (rAAV2/2[MAX]) constitutively expressing separate fluorescent reporters: DHFR fused to yellow fluorescent protein (DHFR.YFP) and mCherry. TMP or vehicle was administered to mice via oral gavage, drinking water, or eye drops. Ocular TMP levels post treatment were quantified by LC-MS/MS. Protein abundance was measured by fundus fluorescence imaging and western blotting. Visual acuity, response to light stimulus, retinal structure, and gene expression were evaluated after long-term (3 months) TMP treatment.

Results. Without TMP, DHFR.YFP was efficiently degraded in the retina. TMP achieved ocular concentrations of ~13.6 μM (oral gavage), ~331 nM (drinking water), and ~636 nM (eye drops). Oral gavage and TMP eye drops stabilized DHFR.YFP as quickly as 6 hours, whereas continuous TMP drinking water could stabilize DHFR.YFP for ≥3 months. Stabilization was completely and repeatedly reversible following removal/addition of TMP in all regimens. Long-term TMP treatment had no impact on retina function/structure and had no effect on >99.9% of tested genes.

Conclusions. This DHFR-based conditional system is a rapid, efficient, and reversible tool to effectively control protein expression in the retina.

Keywords: gene therapy, chemical biology, inducible, DHFR, trimethoprim

Conventional gene therapy approaches utilize constitutive gene expression to combat ocular diseases such as Leber's congenital amaurosis (LCA),[1] choroideremia,[2] MERTK-associated retinitis pigmentosa,[3] amongst others.[4] While appropriate in certain contexts, such as for restoring genes that are incapacitated by loss-of-function mutations or premature stop codons, constitutive ectopic gene expression does bear the potential risk of unanticipated side effects due to sustained, elevated expression in a nonphysiologic (and potentially disadvantageous) manner.[5–7] These risks are especially problematic when attempting to control cellular signaling pathways responsible for promoting protein homeostasis such as the unfolded protein response, oxidative stress response, inflammation and autophagy, all of which are incontrovertibility linked to incurable eye diseases.[8–13] However, the technical capability to regulate these signaling pathways in a physiological context (i.e., conditional sinusoidal expression) and under spatial and temporal control is lacking. Therefore, there is an urgent need to develop and validate a conditional and reversible therapeutic strategy that allows for experimental control of the timing and extent of production of a protein of interest (e.g., a stress-responsive transcription factor) in the eye.

The most commonly used conditional gene therapy approach relies on the tetracycline/doxycycline (tet/dox)-inducible system. While this inducible system has been validated and utilized successfully in the mouse eye,[14–16] it is not an ideal approach for reversibly and repeatedly regulating protein abundance. Firstly, tet/dox systems regulate gene expression at the transcriptional level, requiring subsequent protein translation, which takes additional processing time. Secondly, mouse in vivo tet/dox reversibility experiments typically use a 1- to 2-week induction "on" period for full activation, followed by a 1- to 3-week washout "off" period for full reversibility.[17–20] Furthermore, particular tet/dox systems have been found to be leaky in vivo[21] (although headway has been made in this regard[22]), and high levels of tetracyclines have been suggested to disrupt mitochondrial homeostasis.[23,24]

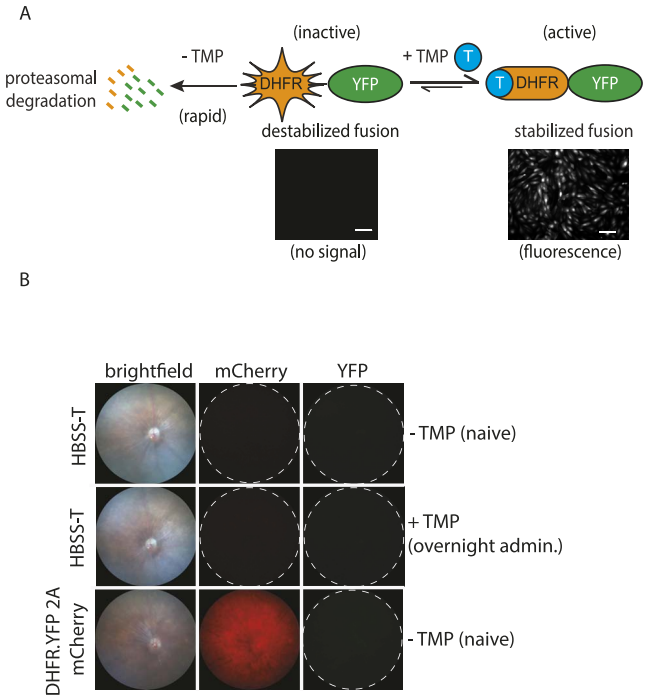

Figure 1. Destabilized DHFR efficiently promotes the degradation of YFP in the absence of TMP. (**A**) Overview of the DHFR-based destabilizing domain approach for controlling protein abundance. In the absence of the small molecule pharmacologic stabilizer, TMP, cells degrade DHFR along with its fusion protein, YFP, via ubiquitin-mediated proteasomal degradation. After addition of TMP, DHFR.YFP is stabilized and fluoresces. Example microscopy images provided are of ARPE-19 cells, which stably express DHFR.YFP[30] and are for illustrative purposes. (**B**) Brightfield and fluorescent fundus images of vehicle (HBSS-T) or rAAV-injected mice (DHFR.YFP 2A mCherry) before TMP treatment ("- TMP"), or after overnight TMP drinking water (0.4 mg/mL, "+ TMP (O/N)"). Representative images of $n \geq 3$ individual mice. *Dashed circles* indicate the area where fluorescent signal would be expected based on brightfield images.

Finally, the tet/dox system itself (i.e., the tet-repressor [TR] or reverse tet-activator [rTA], along with its accompanying promoter) occupies significant additional space within a viral genome, thereby limiting the amount of genetic material that can be packaged in a virus such as recombinant adeno-associated virus (rAAV).

A potentially more efficient, alternative approach to tet/dox-mediated transcriptional regulation would be to directly and conditionally regulate protein abundance with a small molecule. Wandless and colleagues[25,26] have developed two such approaches. The basis for their strategy is the generation of a "destabilizing domain," which is essentially a mutated, inherently unstable protein that is readily ubiquitinated and quickly degraded by the proteasome (Fig. 1A). However, in the presence of a small molecule pharmacologic chaperone, newly synthesized destabilizing domains are properly folded and stabilized at higher steady-state levels within the cell. Thus, in theory, any protein that is covalently fused to the destabilizing domain will be regulated by the degradation kinetics of that domain. Therefore, with simple addition of a small molecule, one can positively regulate protein abundance of the destabilizing domain fusion protein and potentially control any number of cellular signaling pathways in vitro[27–30] or in vivo[26,31–33] In this study, we focused on exploring how well one of these destabilizing domains, a mutated form of *Escherichia coli* dihydrofolate reductase (DHFR),[26] could regulate the abundance of a model fusion substrate, yellow fluorescent protein (YFP) in the mouse eye. We chose this destabilizing domain primarily because of its small molecule chaperone (stabilizer), trimethoprim (TMP). TMP is a highly specific, well-characterized antibiotic drug that normally prevents bacterial growth through inhibition of folate synthesis.[34] TMP has been demonstrated to cross the blood-brain barrier and has been used safely as an antibiotic in humans both in therapeutic and long-term prophylactic regimes for over 50 years.[35]

Herein we demonstrate that DHFR.YFP protein abundance can be quickly and reversibly stabilized in vivo in the mouse eye by multiple different routes of TMP administration, each giving a unique stabilization profile and advantage. Stabilization of DHFR.YFP was surprisingly quick (within 6 hours of TMP administration), predictable (based on intraocular TMP quantification), and completely reversible. If desirable, TMP can promote DHFR.YFP stabilization for $\geq$3 months. Furthermore, long-term (3 months) treatment of mice with TMP had no effect on visual acuity, electroretinogram recordings, retinal morphology, and minimal effects on gene expression (significantly altering 7 out of 22,206 analyzed genes). We envision that this generalizable DHFR-based strategy will enable gene therapy approaches that allow for spatial and temporal flexibility while minimizing potential adverse side effects due to constitutive gene expression.

Materials and Methods

Mouse Use

All animal experiments followed the guidelines of the ARVO Statement for the Use of Animals in Ophthalmic and Vision Research and were approved by the Institutional Animal Care and Use Committee (IACUC) of UT Southwestern Medical Center, Dallas, Texas. C57BL/6J mice were purchased from the UT Southwestern Mouse Breeding Core. Mice were genotyped to confirm the absence of the potentially confounding *rd8* mutation.[36] Equal numbers of age-matched, littermate male and female mice were used whenever possible. Mice were provided standard laboratory chow and allowed free access to water, unless otherwise stated, in a climate-controlled room with a 12-hour light/12-hour dark cycle.

Plasmid and rAAV Generation

A single rAAV construct was used for these studies. This plasmid encodes a constitutively expressed destabilized *E. coli* DHFR fused to hemagglutinin (HA)-tagged YFP followed by a self-cleaving porcine teschovirus (P2A) peptide and mCherry, hereafter called DHFR.YFP 2A mCherry. Thus, due to the P2A peptide, after cleavage, DHFR.YFP contained 22 additional C-terminal amino acids (TGSGATNFSLLKQAGDVEENPG), whereas mCherry contained six additional N-terminal amino acids (PRLQTR). Gene expression was driven by a truncated, chimeric CMV-chicken β-actin promoter (smCBA) and the construct packaged into a capsid mutant rAAV2/2-based vector (termed herein, rAAV2/2[MAX]) containing five single amino acid substitutions (Y272F, Y444F, Y500F, Y730F, T491V) and a peptide insertion (N587_R588insLALGETTRPA) that has been shown recently to have significantly enhanced photoreceptor transduction following intravitreal injection (Supplementary Fig. 1A).[37] Virus was purified by iodixanol gradient as described previously.[38]

Intravitreal Injections

Ten- to twelve-week-old C57BL/6J mice were anesthetized with a ketamine/xylazine cocktail (120 mg/kg, 16 mg/kg, respec-

tively) followed by pupil dilation using tropicamide (1% [w/v]) and phenylephrine hydrochloride (2.5% [w/v]), both from Alcon, Fort Worth, Texas. Alcaine (0.5% [w/v], Alcon) was used to locally anesthetize the eye followed by application of GenTeal eye gel (severe dry eye formula, Alcon) to prevent corneal drying. Intravitreal injections were guided by the use of a Stemi 305 stereo microscope (Zeiss, Oberkochen, Germany). Briefly, the right eye was slightly proptosed by periocular pressure and a 33G ½" needle with a 10 to 12° bevel fitted to a Hamilton micro syringe (Hamilton, Reno, NV, USA) was inserted just below the limbus at a ~45° angle. Two microliters of rAAV (7.6×10^9 viral genomes) was slowly injected into the vitreous over the course of ~1 minute. For the left eye, the same injection procedure was followed, but using vehicle (Hanks' Balanced Salt Solution with 0.14% Tween [HBSS-T]). Postinjection, a drop of GenTeal and a small amount of AK-POLY-BAC antibiotic ointment (Akorn, Lake Forest, IL, USA) were applied to the eye. Forty-eight hours after injection, mice were macroscopically inspected and those with any apparent ocular damage (e.g., cloudy eye) were not used for subsequent experiments.

Fundoscopy

In vivo retina imaging was initially performed ≥3 weeks after rAAV injection using a fundus camera (Micron IV, Phoenix Research Laboratories, Pleasanton, CA, USA) to assess proper rAAV expression (mCherry signal) and regulation of DHFR.YFP proteolysis (lack of YFP signal). Briefly, under ketamine/xylazine anesthesia, both eyes were dilated as described above before imaging. GenTeal gel was applied to the cornea to prevent drying and to obtain a clear image of the retina and optic nerve. Brightfield and fluorescent (ex/em: 485/525 nm for YFP; 554/609 nm for mCherry) images were recorded. Light intensity (1/4 of maximum) and electronic gain (12 db) for all images were initially set based on obtaining no observable mCherry or YFP background signal in HBSS-T-injected eyes. Subsequent fundus images were obtained at the indicated time points thereafter as described below.

TMP Administration

Three different routes of TMP administration were used: (1) oral gavage, (2) drinking water, and (3) eye drops. To administer TMP as a single, temporally controllable bolus, mice were given TMP by oral gavage. TMP (Sigma-Aldrich Corp., St. Louis, MO, USA) was freshly dissolved in 100% DMSO (Fisher Chemicals, Fair Lawn, NJ, USA) at a concentration of 140 mg/mL and diluted 10-fold in a solution of 20% PEG400 (Fisher Chemicals), 2% Tween 80 (Fisher Chemicals), 10% cremaphor (Sigma-Aldrich Corp.), and 58% dextrose (Fisher Chemicals) in nanopure water. Mice were given 200 µL of this solution, which equates to 2.8 mg TMP/mouse/dose. For drinking water experiments, 400 mg TMP was dissolved in 1 L standard drinking water (0.4 mg/mL final). This dose amounts to ~2.5 mg/mouse over a 24-hour period (most of which is drunk during the night) according to previous imbibing estimates of ~6.25 mL/day for a C57BL6/J mouse.[39] Drinking water TMP was changed weekly and periodically mixed during the course of the experiments. No aversion to TMP drinking water was noted, even with prolonged treatment. Finally, TMP was administered via eye drops to avoid systemic exposure. Polytrim (10,000 units/mL polymyxin B sulfate, 1 mg/mL TMP, Allergan, Dublin, Ireland) was administered through six hourly eye drops (~20 µL/drop) for a total dose of ~120 µg of TMP. Note: as mice are coprophagous, during "washout" periods without TMP, we believe it is important to move mice to a new, fresh cage to minimize potential reintroduction of TMP through excreta or the inadvertent consumption of soiled bedding.

TMP Quantification

At each indicated time point, 8- to 10-week-old mice ($n \geq 3$) were euthanized by an overdose of ketamine/xylazine and their eyes were enucleated. The anterior chamber was dissected and discarded. Neural retina were peeled from the RPE and snap frozen in liquid nitrogen. For particular experiments, whole blood was collected by cardiac puncture in acid citrate dextrose (ACD)-coated syringes. Blood was spun for 10 minutes at 10,000 rpm and the clear layer of plasma was collected. Retina and plasma samples were stored at –80°C until submission to the UT Southwestern Preclinical Pharmacology Core. Retina tissue and/or plasma were analyzed for TMP concentration using a liquid chromatography-tandem mass spectrometry (LC-MS/MS) method. Retinas were homogenized in PBS using a BeadBug (Benchmark Scientific, Atkinson, NH, US) microtube homogenizer with 3.0 mm Zirconium beads (Benchmark Scientific). For standards, blank commercial plasma (Bioreclamation, Westbury, NY, USA) or untreated brain tissue homogenate was spiked with varying concentrations of TMP. Standards and samples were mixed with 3× volume of acetonitrile containing formic acid and an internal standard (tolbutamide, Sigma-Aldrich Corp.), vortexed, and then spun 5 minutes at 16,100*g*. Supernatant was removed and spun again and the resulting second supernatant was put into an HPLC vial and analyzed by LC-MS/MS using a SCIEX (Framingham, MA, USA) 4000-QTRAP coupled to a Shimadzu Prominence LC (Columbia, MD, USA). TMP was detected with the mass spectrometer in multiple reaction monitoring (MRM) mode by following the precursor to fragment ion transition 291.1 → 230.0. An Agilent Zorbax XDB-C18 column (50 × 4.6 mm, 5 mm packing, Santa Clara, CA, USA) was used for chromatography with the following conditions: Buffer A: dH20 + 0.1% formic acid, Buffer B: MeOH + 0.1% formic acid, 1.5 mL/min flow rate, 0 to 1.5 minutes 3% B, 1.5 to 2.0 minutes gradient to 100% B, 2.0 to 3.5 minutes 100% B, 3.5 to 3.6 minutes gradient to 3% B, 3.6 to 4.5 minutes 3% B. Tolbutamide (transition 271.2 → 91.2) was used as an internal standard. Back-calculation of standard curve and quality control samples were accurate to within 15% for standards and quality controls for 85% to 100% of these samples at concentrations ranging from 0.1 ng/mL to 500 ng/mL. A Grubb's Test (GraphPad QuickCalcs, San Diego, CA, USA) was used to test for significant outliers in TMP concentrations in the different treatment groups.

Fundus Imaging Quantification

For quantification purposes, all fluorescent fundoscopy images were first split into red (for mCherry) and/or green channels (for DHFR.YFP) using ImageJ software (ImageJ, version 1.51H). A circle area tool was used to draw a border around the fluorescent signal (or where the fluorescent signal should appear, as in the case of TMP naïve or TMP withdrawal mice) to obtain the average pixel intensity. Background fluorescent signal (defined as the average signal intensity in the YFP or mCherry channel in HBSS-T-injected mice) was subtracted from all images of virus-injected eyes, and the DHFR.YFP/mCherry signal ratio for each treatment and different route of administration is presented.

Western Blotting

Neural retina were extracted and snap frozen in liquid nitrogen, then stored at –80°C until use. Individual retina were homogenized in ice-cold radioimmunoprecipitation assay buffer (Santa Cruz, Dallas, TX, USA) supplemented with

Investigative Ophthalmology & Visual Science

protease inhibitors (Halt Protease Inhibitor Cocktail, ThermoFisher Scientific, Waltham, MA, USA) and benzonase (Sigma-Aldrich Corp.). Samples were then incubated on ice for 10 minutes and spun at 15,000 rpm for 10 minutes at 4°C. Supernatants were collected and assayed for protein concentration by a bicinchoninic acid assay (Pierce, Rockford, IL, USA). Forty micrograms of protein was separated on a 4-20% Tris glycine gel, followed by transfer to a nitrocellulose membrane using a G2 blotter. Uniform protein loading was confirmed by Ponceau S, and blots were blocked with Odyssey Blocking Buffer (LI-COR, Lincoln, NE, USA) for 1 hour at room temperature (RT). Primary antibodies were diluted in 5% BSA in Tris-buffered saline (TBS); anti-HA (1:1500, clone 2-2.2.14, Pierce) and anti-β; actin (1:1400, cat# 926-42212, LI-COR) were used overnight at 4°C. Species appropriate IR Dye-conjugated secondary antibodies diluted in 5% milk (1:15,000, LI-COR) were incubated on the blots for 40 minutes at RT. Blots were imaged on a LI-COR Odyssey CLx and quantified using Image Studio software (LI-COR).

Visual Acuity

To evaluate whether visual acuity was altered at any point during TMP administration (0.4 mg/mL, drinking water), we evaluated the optokinetic reflex of the mice at 1, 3, 5, 7, and 12 weeks (3 months) post treatment ($n \geq 3$ control, ≥ 3 TMP treated) using a virtual optomotor system[40] (OptoMotry; Cerebral Mechanics, White Plains, NY, USA). The spatial frequency threshold was assessed in freely moving mice and measured at maximum contrast (100%) by using a staircase method beginning with a minimum preset frequency of 0.050 cycles/degree. The thresholds were identified as the highest values that still elicited a following response in the mouse. Spatial frequency for each mouse was averaged for two trials after a minimum interval of 3 hours for each mouse.

Electroretinogram

The effect of TMP on retina function was evaluated by full field ERG (Ganzfeld ERG, Phoenix Instruments, Pleasanton, CA, USA). Briefly, a cohort ($n \geq 3$) of 10-week-old mice were given TMP (0.4 mg/mL in drinking water, "+ TMP") or normal drinking water ("- TMP") for 3 months. Mice were dark-adapted overnight followed by anesthetization with ketamine/xylazine and pupil dilation (performed under dim, indirect red-light conditions). A gold recording electrode was placed on one eye and needle electrodes were placed subcutaneously into the scalp (reference), and in the tail (ground). A series of full-field flash stimuli ranging from −1.7 to 3.1 log cd*s/m^2 were presented to the eye by a Ganzfeld dome. As the light intensity increased, the interstimulus interval increased from 7 to 75 seconds, and the flashes were averaged to generate a waveform for each flash intensity. The analysis of the voltage tracings was accomplished using LabScribe software (Phoenix Research Labs).

Metabolic Phenotyping

To assess for any differences in body composition after long-term TMP administration, mice were analyzed using a Bruker minispec LF90 (Bruker Optics, Billerica, MA, USA) prior to, and after 3 months of TMP (0.4 mg/mL in drinking water, $n = 4$) or normal water treatment ($n = 4$). This system accurately measures total body mass, fat mass, lean tissue mass, free water, and total body water. Each mouse was scanned twice per session and these values were averaged prior to analysis.

Immunohistochemistry (IHC) and Hematoxylin and Eosin (H&E) Staining

Mice were euthanized by ketamine/xylazine overdose. Eyes were rapidly enucleated and processed for freeze substitution according to Sun et al.[41] with slight modification. Enucleated eyes were submerged in chilled isopentane for 1 minute then rapidly transferred to chilled 97% methanol and 3% acetic acid (MAA) and stored at −80°C for 48 hours. After 48 hours, the vial was warmed stepwise to −20°C for 24 hours, followed by 4°C for 4 hours, and then RT for 2 hours. MAA was then replaced with 100% ethanol and the eye was processed into paraffin-embedded sections (Histo Pathology Core, UT Southwestern). H&E staining was performed by the Histo Pathology core and images of the sections were taken at 40× magnification on either side of the optic nerve head using an inverted epifluorescent microscope (Zeiss).

For IHC, HBSS-T and virus-injected eyes were processed into paraffin-embedded sections as described above. The unstained paraffin sections were deparaffinized and the antigen was retrieved by heat-induction and sodium citrate treatment. Antigen-retrieved sections were blocked with 5% goat serum (in PBS, 0.1% Triton-X 100, 1 hour at RT), then incubated overnight at 4°C with or without (for the secondary only control) primary antibody (rabbit anti-mCherry, 1:100, ab167453, Abcam, Cambridge, United Kingdom). Sections were washed three times in PBS-T and incubated with secondary antibody (anti-rabbit AlexaFluor 488, 1:1000, Life Technologies, Carlsbad, CA, USA) for 1 hour, washed with PBS-T and then stained with Hoescht for 20 minutes. After a brief wash of 10 minutes in PBS-T, sections were mounted with ProLong Diamond (Life Technologies). Images were taken at 40× magnification using an inverted epifluorescent microscope (Zeiss).

Whole Transcriptome Profiling and Quantitative Real-Time PCR (qPCR)

After ketamine/xylazine overdose, eyes were enucleated and immediately dissected. The neural retina were peeled from the eye cup and flash frozen. Tissues were kept at −80°C until RNA extraction. Samples were homogenized in 350 μL of lysis buffer (Bio Rad Aurum Total RNA Mini Kit, BioRad, Hercules, CA, USA) with an Eppendorf-based mortar and pestle. After homogenization, RNA was extracted as described previously.[42,43] Samples ($n = 4$ "- TMP", $n = 4$ "+ TMP") were eluted in 40 μL of RNase/DNase-free water, submitted to the Genomics and Microarray Core (UT Southwestern), quality checked (TapeStation, Aglient, Santa Clara, CA, USA), and run using a mouse Clariom S whole transcriptome chip (Life Technologies). Data were analyzed using Transcriptional Analysis Console software (Life Technologies) using cutoffs of $\geq$ 2-fold change (compared to "- TMP" control samples) and a *P*-value of <0.01. To confirm the microarray results, ~80 ng of mRNA was reverse transcribed into cDNA using qScript cDNA SuperMix (Quanta Bioscience, Beverly, MA, USA). cDNA was diluted 20-fold in water and analyzed by TaqMan assays on a QuantStudio6 (Life Technologies). The following probes were used along with TaqMan Advanced Fast master mix (all from Life Technologies): β-*actin* (Mm02619580), *Bgn* (Mm01191753), *Hba-a1/2* (Mm02580841), *Hbb-bs/t* (Mm03646870), and *Skint7* (Mm03807349).

Statistics

All experiments were performed using ≥3 mice per experiment/time point. To determine significance for differences in TMP concentrations, fundus image quantification, western

Investigative Ophthalmology & Visual Science

blotting, visual acuity, ERG, and metabolic profiling, an unpaired 2-tailed *t*-test assuming equal variance was used. For microarray experiments, significance was automatically calculated using the Transcriptional Analysis Console software. For qPCR validation assays, an unpaired 1-tailed *t*-test was used assuming equal variance and comparing the values to a hypothetical mean of 1 (i.e., unchanged). Values were determined to be significant when *P* values were less than 0.05.

Results

DHFR.YFP Is Effectively Degraded in Mouse Retina in the Absence of TMP

We first evaluated whether destabilized DHFR.YFP was effectively turned-over by the proteasome in mouse retina in the absence of the DHFR inhibitor, and small molecule stabilizing ligand, TMP (see Fig. 1A illustration). rAAV2/2[MAX] smCBA DHFR.YFP 2A mCherry was intravitreally injected into 10- to 12-week-old C57BL/6J mice followed by a ≥3-week incubation period to allow transgene expression. Intravitreal injection of the rAAV2/2[MAX] capsid mutant serotype vector has been previously shown to result in high levels of transgene expression throughout the neural retina with enhanced photoreceptor transduction (Supplementary Fig. 1A).[37] Brightfield and fluorescent fundus images were then taken to evaluate the retina and gauge the levels of the fluorescent reporters. No background fluorescence signal was observed in the control, HBSS-T-injected mice in the presence or absence of TMP (Fig. 1B). rAAV-injected mice displayed only strong mCherry signal with no detectable YFP signal in the absence of TMP (Fig. 1B), suggesting that the destabilized DHFR.YFP fusion protein is effectively degraded.

DHFR.YFP Protein Abundance Is Quickly Stabilized Using Orally-Delivered TMP and Stabilization Is Reversible

Prior in vivo studies using destabilized DHFR to control protein abundance in the rodent brain have relied on phenotypic changes or levels of fusion proteins to assess whether orally administered TMP actually reaches the striatum over the course of a 3-week regimen.[26,32] While it is reasonable to assume that if TMP can enter the brain, it can also reach the eye, to the best of our knowledge, quantification of TMP in the mouse eye after administration has not been attempted previously. Therefore, we gave mice TMP via oral gavage (2.8 mg in 200 µL), harvested their neural retina, and quantified the amount of TMP in the tissue using LC-MS/MS. We found that 6 hours after TMP administration, high levels of TMP could be easily detected in the mouse eye (4.2 ± 1.6 mg of TMP/g of tissue; Fig. 2A); a timeframe that was much quicker than previously appreciated in vivo. Assuming an approximate high-end vitreous volume of 5.3 µL,[44] and an average neural retina weight of 5 mg, this TMP concentration amounts to ~13.6 µM, a level well above the maximal concentration used for even cell culture experiments to fully stabilize DHFR fusions[29,30]; typically 1 µM. Next we performed washout experiments 24 hours to 9 days post initial gavage to assess how quickly TMP was metabolized in the eye. We were surprised to find that even 120 hours after gavage, TMP could still be detected at levels that should stabilize DHFR (39.3 ± 13.6 ng/g, ~127 nM; Fig. 2A). Based on these observed TMP concentrations, we predicted that ~9 days of washout would be needed to reduce ocular TMP levels to below those required for reliable DHFR stabilization (<~25 nM, Fig. 2A). Interestingly, the levels of TMP in the eye appear to be longer lasting than those observed in the plasma (Supplementary Fig. 1B), potentially due to metabolism of TMP in the liver, or because of its susceptibility for kidney filtration and excretion via urine when found in blood.

Subsequently, we confirmed TMP administered by gavage stabilized DHFR.YFP protein levels in a predictable fashion that paralleled observed ocular TMP levels. Six hours after initial gavage, we detected a robust and significant increase in DHFR.YFP signal ("+ TMP (6 hours post administration)"; Figs. 2B, 2C), which persisted for at least 72 hours post gavage ("+ TMP (72 hours post administration)"; Figs. 2B, 2C). However, 9 days after initial TMP treatment, no DHFR.YFP signal could be detected in fundus images, and DHFR.YFP signal was not significantly different from TMP naïve mice ("+ TMP (9 days post administration)"; Figs. 2B, 2C). Importantly, re-stabilization of DHFR.YFP was significantly increased within 6 hours of TMP re-administration by gavage ("+ TMP (6 hours post re-administration)"; Figs. 2B, 2C). The dependence of DHFR.YFP protein abundance on the presence or absence of TMP was orthogonally confirmed by western blotting of neural retina extracts 6 hours after TMP (or vehicle) gavage treatment (Figs. 2D, 2E). In rAAV-injected mice, in the absence of TMP, a very faint amount of degraded DHFR.YFP product was observed, indicating a minimal degree of "leakiness" (Figs. 2D, 2E). DHFR.YFP protein levels were significantly elevated in the presence of TMP (Figs. 2D, 2E). Full western blot lanes are shown in Supplementary Fig. 1C.

DHFR.YFP Protein Levels in the Eye Can Be More Efficiently Stabilized and Destabilized Using TMP Administered in Drinking Water

While TMP administration by gavage served as proof-of-principle demonstration that DHFR.YFP abundance can be stabilized very quickly in the retina, elevated stabilizing levels of TMP in the eye persisted over a span of multiple days. This regimen would not be ideal for certain gene therapy strategies that require quicker "on/off" kinetics. Thus, we explored alternative means of delivering TMP to the eye. Mice were given a saturated amount of TMP (0.4 mg/mL) in their drinking water overnight (14–16 hours), which equates to a total of ~2.5 mg, assuming an average drinking rate of ~6.25 mL/day for a C57BL6/J mouse,[39] a total dose similar to that administered by gavage. Overnight administration of TMP resulted in 102 ± 44 ng of TMP/g of neural retina (Fig. 3A). This concentration amounts to ~331 nM, a concentration sufficient to fully stabilize DHFR.YFP in cell culture experiments.[30] After overnight removal of TMP, ocular TMP levels fell dramatically (to 8.3 ± 1.9 ng/g, ~26.8 nM) and were not significantly different from control, untreated eyes (Fig. 3A). These results were also confirmed in corresponding plasma samples of treated/untreated mice (Supplementary Fig. 1D).

As expected, based on the observed ocular TMP levels, DHFR.YFP protein levels were predictably and significantly stabilized after overnight TMP administration ("+ TMP (overnight administration)"; Figs. 3B, 3C), and destabilized to TMP naïve (i.e., background) levels after overnight withdrawal and replacement with normal drinking water ("- TMP (overnight withdrawal)"; Figs. 3B, 3C). DHFR.YFP can be re-stabilized in a significant fashion repeatedly as necessary ("+ TMP (overnight re-administration)"; Figs. 3B, 3C), and if longer-term stabilization is required, sustained administration of TMP in drinking water can promote DHFR.YFP stability for ≥3 months ("+ TMP (3 months constant)"; Fig. 3B). Moreover, 1 month of DHFR.YFP stabilization can be simply reversed by a 40-hour washout period when no TMP is provided and is replaced by normal drinking water ("- TMP (40-hour withdrawal)"; Figs. 3B, 3C).

Investigative Ophthalmology & Visual Science

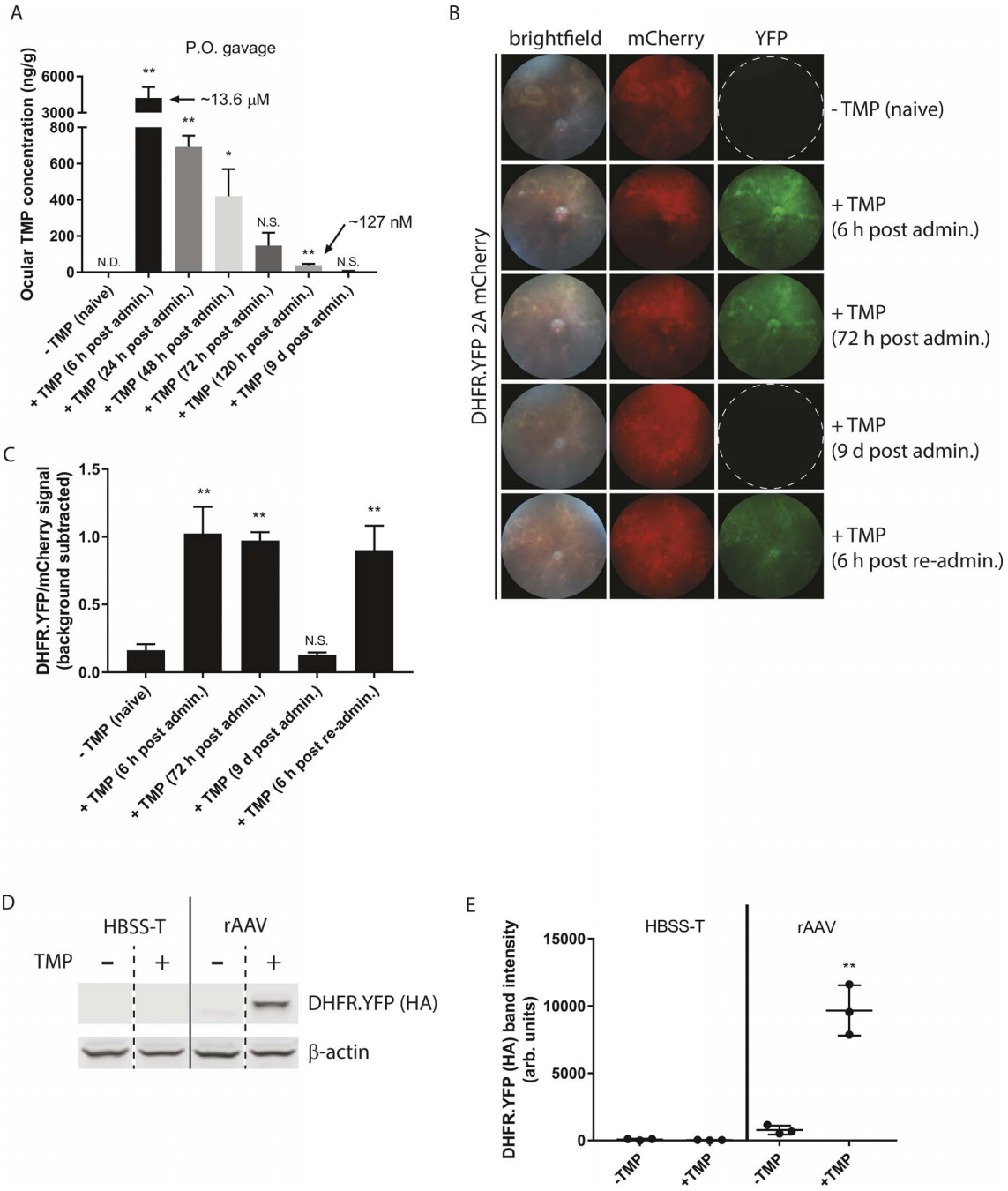

Figure 2. Oral gavage-administered TMP readily enters the eye and stabilizes DHFR.YFP. (**A**) Quantification of TMP in neural retina samples after oral gavage. Mice were given a bolus of 2.8 mg of TMP and their neural retina were analyzed 6 hours later ("+ TMP (6 hours post administration)") or 24 hours to 9 days later ("+ TMP (24 hours to 9 days post administration)"). $n \geq 3$, mean ± S.D. (**B**) Fundus images of rAAV-injected mice at the indicated time points corresponding to TMP treatment. A single mouse was used for all images shown in (**B**). All images are representative of $n \geq 3$ individual mice. (**C**) Quantification of fundus images shown in (**B**). (**D**) Neural retina western blotting for DHFR.YFP (using the HA tag antibody) or β-actin 6 hours after TMP oral gavage. Representative image of three individual mice. (**E**) LI-COR quantification of the DHFR.YFP band. $n = 3$, mean ± SD. ND, not detected; NS, not significant; $^{*}P < 0.05$; $^{**}P < 0.01$, unpaired, 2-tailed *t*-test assuming equal variance compared to "- TMP (naïve)" samples in (**A**) and (**C**) and rAAV-injected "- TMP (naïve)" samples in (**E**).

TMP Eye Drops Can Quickly and Non-systemically Control DHFR.YFP Abundance

As TMP is an *E. coli*-specific bacteriostatic antibiotic that inhibits folate synthesis, and administering TMP systemically could alter the gut microbiota, we also administered TMP through the use of commercially available eye drops to avoid systemic effects of TMP in mice. Although the total amount of TMP that could be easily administered via eye drops (120 μg) was over 20-fold smaller than the amount of TMP delivered by either gavage or drinking water, we found a substantial amount of TMP in the neural retina 6 hours after administration (196 ± 123 ng/g; Fig. 4A). This amount corresponds to an average concentration of ~636 nM, ~1.9 times the TMP levels observed after overnight administration in drinking water. As these ocular TMP levels were initially higher than those found

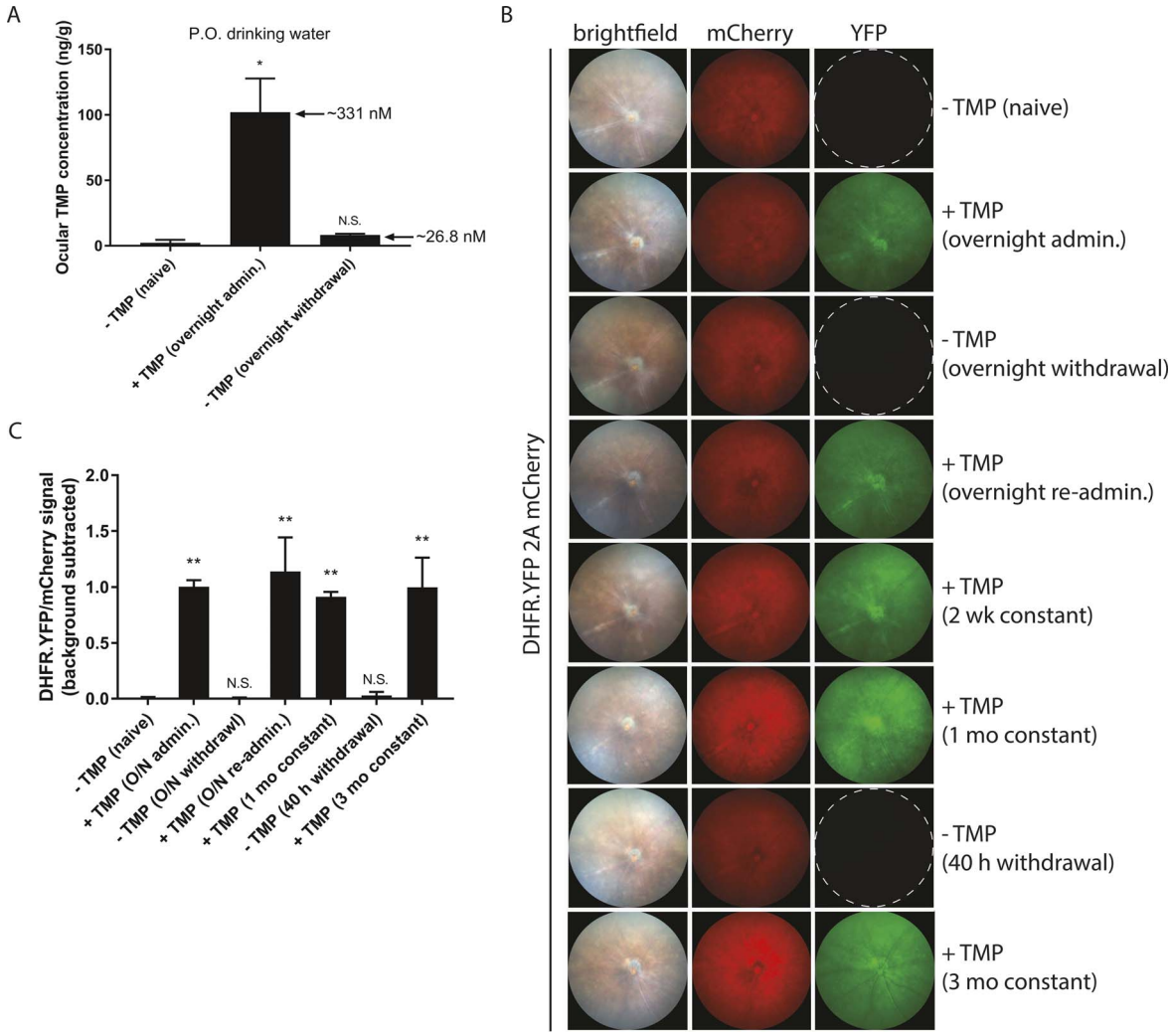

Figure 3. Drinking water containing TMP can reliably stabilize DHFR.YFP as quickly as overnight, or for ≥ 3 months. (**A**) Quantification of TMP in neural retina samples after overnight (14–16 hours) addition ("+ TMP (overnight administration)"), or addition then removal of 0.4 mg/mL TMP and replacement with normal water ("- TMP (overnight withdrawal)"). $n \geq 3$, mean ± SD. (**B**) Fundus images of rAAV-injected mice at the indicated time points corresponding to TMP treatment. A single mouse was used for all images shown in (**B**), except for the 3 month constant TMP mouse. Images are representative of $n \geq 3$ individual mice. (**C**) Quantification of fundus images shown in (**B**). NS, not significant; $^*P < 0.05$, unpaired, 2-tailed *t*-test assuming equal variance compared to "- TMP (naïve)" samples in (**A**) and (**C**).

with drinking water-administered TMP, the washout period required for TMP to fall below stabilizing levels was also longer (48 hours; Fig. 4A). In accordance with the observed ocular TMP levels post eye drop administration, stabilization of DHFR.YFP again followed a predictable pattern, allowing for significant stabilization within 6 hours of administration ("+ TMP (6 hours post administration)"; Figs. 4B, 4C), and destabilization after a 48-hour washout period ("+ TMP (48-hour post administration)"; Figs. 4B, 4C). Finally, DHFR.YFP protein levels could be significantly re-stabilized again within 6 hours after re-administration of eye drops ("+ TMP (6-hour re-administration)"; Figs. 4B, 4C).

Long-Term TMP Treatment (3 Months) Does Not Affect Visual Acuity, ERG Response, Retinal Structure, or Whole-Body Metabolism

Given that TMP administration using three different modalities resulted in robust and predictable stabilization of DHFR in the mouse eye, and thus may serve as a unique and powerful way to therapeutically control protein abundance in the eye, we next wanted to determine if long-term TMP treatment had any impact on visual function/structure or gene expression in the retina. Mice were given TMP in their drinking water (0.4 mg/mL) daily for up to 3 months. During this course of treatment, we used OptoMotry[40] to test visual acuity at 1, 3, 5, 7, and 12 weeks (3 months) after initiating TMP treatment. No significant changes were observed at any time point (Fig. 5A).

We proceeded to assess the effect of TMP treatment on visual function and response to light. Dark-adapted full-field ERG measurements were performed on control (- TMP) or TMP-treated mice (+ TMP). Both a-wave and b-wave amplitudes were measured using progressively increasing intensities and duration of light (Figs. 5B, 5C). No consistent, significant trends were observed between the control and TMP-treated groups (Figs. 5B, 5C).

After 3 months of TMP treatment, mice were also analyzed for any gross anatomical changes in body weight, fat, lean mass or fluid (Bruker minispec LF90, Bruker Optics, Billerica, MA, USA) as potential indications of a poor response to long-term

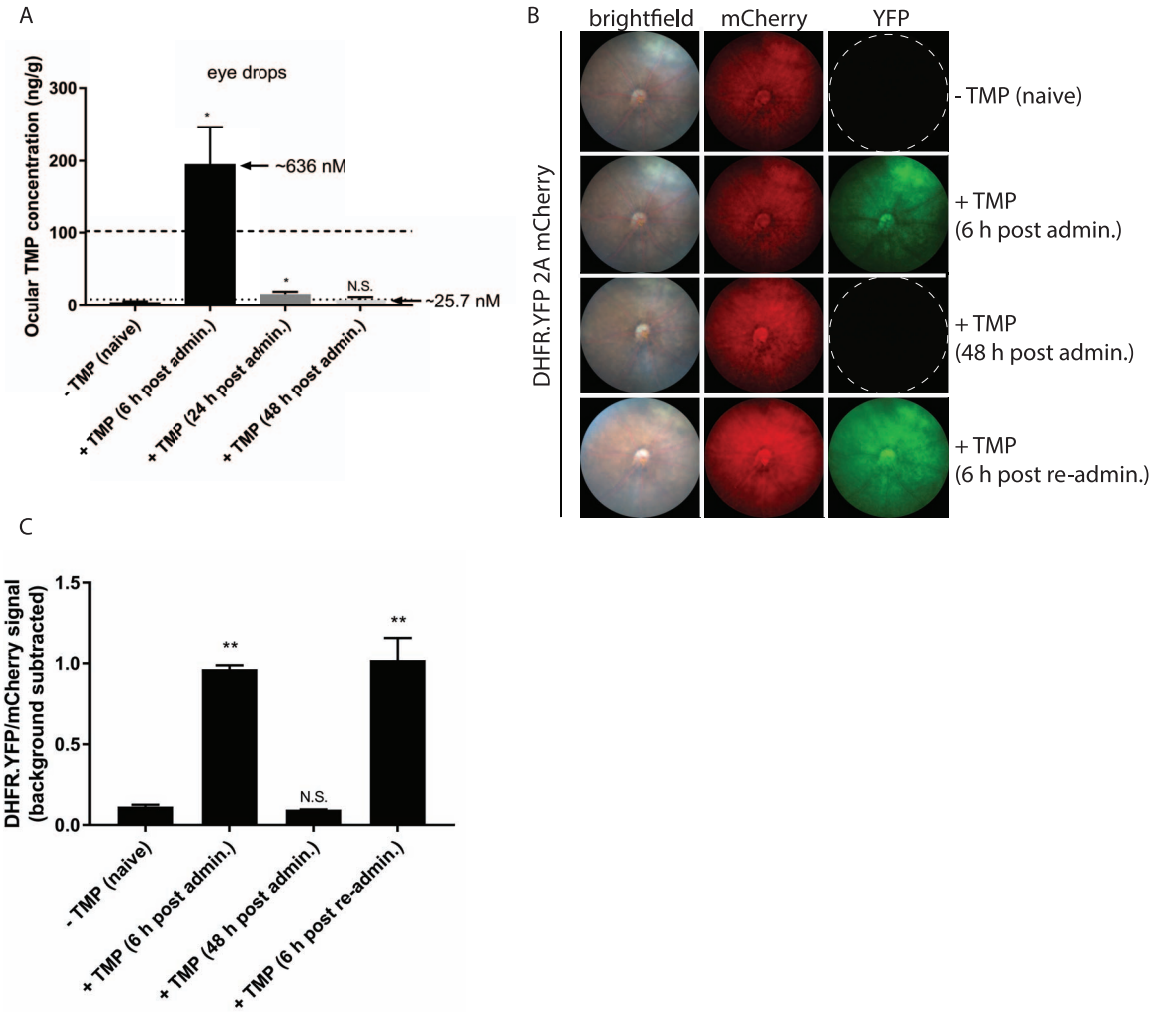

Figure 4. Topically administered TMP eye drops can quickly enter the eye and stabilize DHFR.YFP. (**A**) Quantification of TMP in neural retina samples after six hourly TMP eye drops (one drop/h, "+ TMP (6 hours post administration)") or 24, 48 hours thereafter ("+ TMP (24, 48 hours post administration)"). *Dotted line* corresponds to the "- TMP (overnight withdrawal)" concentration in Fig. 3A, whereas the *dashed line* represents the "+ TMP (overnight administration)" values from Fig. 3A for comparison. $n \geq 3$, mean ± SD. (**B**) Fundus images of rAAV-injected mice at the indicated time points corresponding to TMP treatment. A single mouse was used for all images shown in (**B**), which is representative of $n \geq 3$ individual mice. (**C**) Quantification of fundus images shown in (**B**). NS, not significant; $^*P < 0.05$, unpaired, 2-tailed *t*-test assuming equal variance compared to "- TMP" samples in (**A**) and (**C**).

TMP administration. However, aside from a general increase in total, fat, and lean mass in both groups (due to an increase in the size of the mice with age), no differences were observed between the two groups before or after TMP treatment (Supplementary Fig. 1E). Mice were then euthanized and their eyes were used for a histological retinal comparison. H&E staining of the retina adjacent to the optic nerve demonstrated no difference in total retinal thickness, or disruption of any retinal cell layers (Fig. 5D). Overall, these collective observations indicate that long-term TMP is well tolerated with no observable effects on vision or gross physiology.

Long-Term Treatment With TMP (3 Months) Minimally Affects Gene Expression in the Retina

After 3 months of TMP treatment, mice were euthanized and their neural retina were harvested for total mRNA extraction. Unbiased, transcriptome-wide gene expression changes were evaluated using a mouse Clariom S microarray (>20,000 well-annotated genes). Using conventional ≥ 2-fold, $P < 0.01$ cutoffs, we identified only seven differentially regulated genes (Fig. 6A), a hit rate of 0.0315% (7/22,206 total unique transcripts). Thus, prolonged TMP treatment had no significant effect on >99.9% of the analyzed genes. Interestingly, a cluster of four hemoglobin-related genes were identified to be upregulated with TMP treatment (Fig. 6A). These genes were: hemoglobin α, adult chain 1 (*Hba-a1*, 3.43-fold), hemoglobin α, adult chain 2 (*Hba-a2*, 3.41-fold), hemoglobin β, adult chain s (*Hbb-bs*, 2.69-fold), and hemoglobin β, adult chain t (*Hbb-bt*, 2.52-fold, Fig. 6A, Supplementary Fig. 1D). Biglycan (*Bgn*), a gene involved in tissue growth and regeneration, was also identified as significantly increased in + TMP mice (2.02-fold, Fig. 6A, Supplementary Fig. 1D). Conversely, selection and upkeep of intraepithelial T cells 7 (*Skint7*) and RIKEN cDNA 6330415B21 (*6330415B21Rik*), both poorly characterized genes, were identified as significantly repressed in "+ TMP" neural retina (−2.08 and −2.14 fold, respectively, Fig. 6A, Supplementary Fig. 2A). To confirm the microarray findings, we assayed for gene expression changes using TaqMan assays that rely on unique primer/probe sets that are independent of

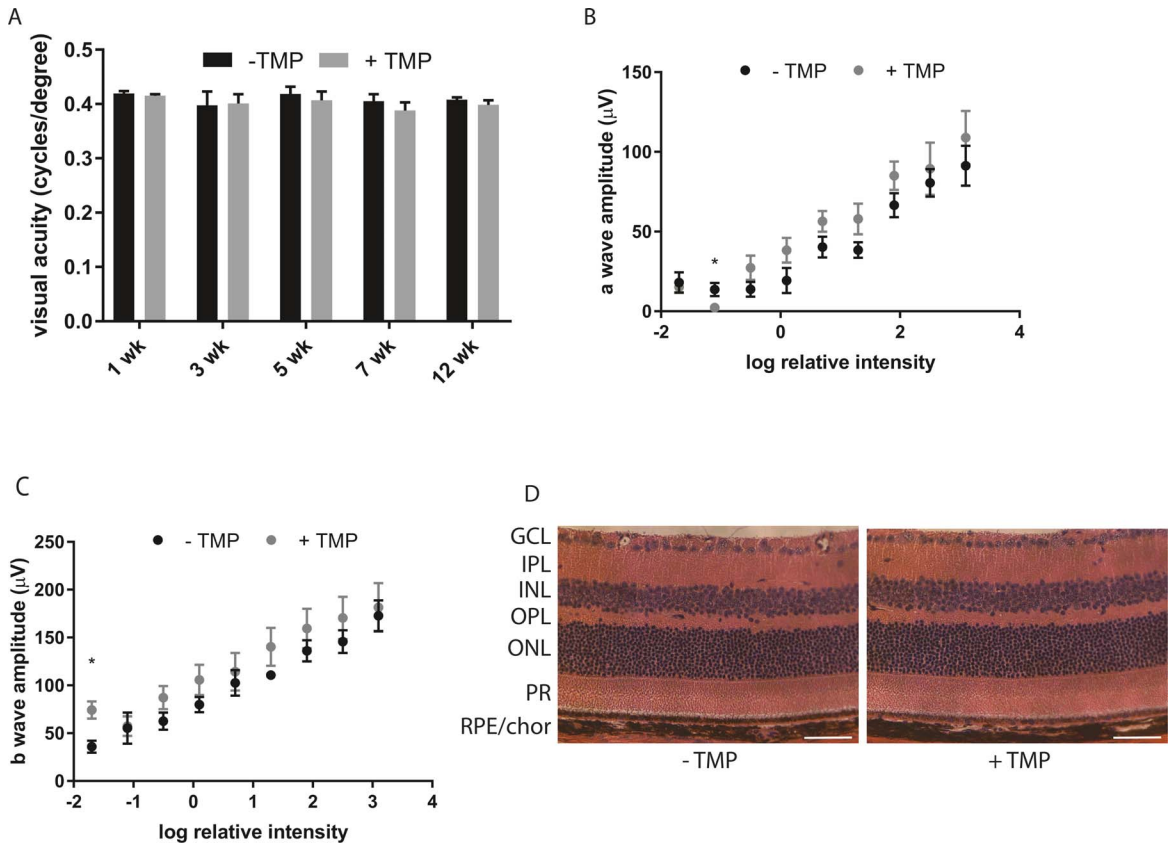

Figure 5. Long-term TMP has no effect on visual acuity, response to light stimulus or retinal structure. (**A**) Visual acuity was evaluated in untreated mice ("- TMP") or mice given TMP drinking water (0.4 mg/mL, "+ TMP") for select intervals up to 12 weeks (3 months). No significant differences were observed at any time point. $n \geq 4$, mean ± SD. (**B**, **C**) Evaluation of full field ERG-evoked responses to increasing light stimulus after 3 months of TMP treatment. No consistently significant trends were observed in either a- or b-wave responses. $n \geq 3$, mean ± SEM. (**D**) Representative H&E staining of freeze-substituted eyes imaged after 3 months of TMP or normal water. $n = 4$; *scale bar*, 50 μm. $^{*}P < 0.05$, unpaired, 2-tailed *t*-test assuming equal variance compared to "- TMP" samples in (**A**–**C**).

those used to perform the microarray experiments (no probe set was available for *6330415B21Rik*). *Bgn* expression levels in "+ TMP" samples were found to not be significantly different than "- TMP" control samples (Fig. 6B), whereas *Skint7* expression levels were undetectable by qPCR (Supplementary Fig. 2B). However, indeed, *Hba-a1/2* and *Hbb-bs/t* expression levels were confirmed to be significantly elevated (1.9 ± 0.2 and 1.5 ± 0.1-fold vs. "- TMP" samples, respectively, Fig. 6B), which may be an indication of folate synthesis disturbances and changes to erythropoiesis.[45]

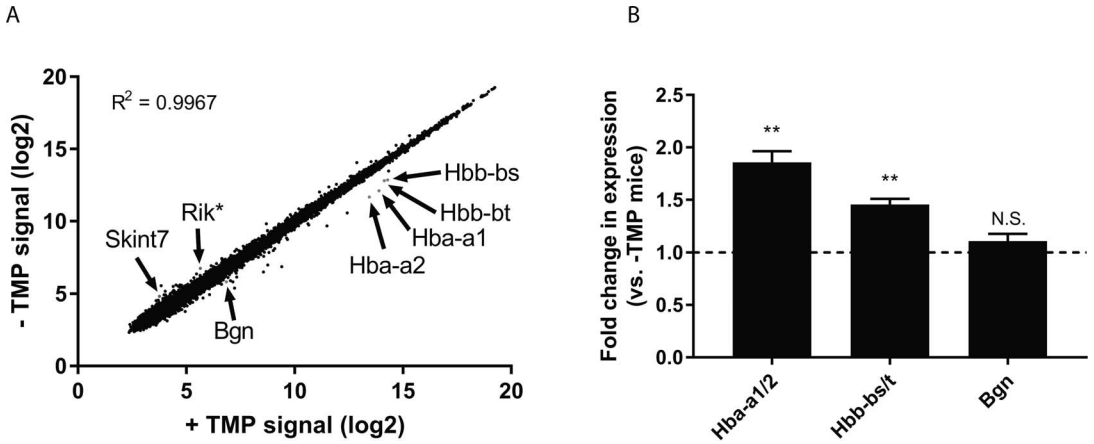

Figure 6. Long-term TMP treatment minimally effects neural retina gene expression. (**A**) Comparison of microarray gene expression profiles from control ("- TMP") and TMP-treated (3 months, 0.4 mg/mL, "+ TMP") neural retina. Genes with ≥ 2-fold higher (*green dots*) or lower (*red dots*) expression than "- TMP", $P < 0.01$ are shown. Linear regression analysis revealed highly correlated values ($r^2 = 0.9967$). *Rik = *6330415B21Rik*. $n = 4$. (**B**) TaqMan probe validation of differentially regulated genes. $n = 4$, mean ± SD. NS, not significant; $^{**}P < 0.01$, one sample unpaired *t*-test assuming equal variance and comparing the values to a hypothetical mean of 1 (i.e., unchanged).

Investigative Ophthalmology & Visual Science

Discussion

Herein we have characterized how a destabilizing version of DHFR can control the abundance of an idealized fusion partner, YFP, in the mouse eye. These studies lay the foundation for using DHFR as a small molecule-regulatable domain for controlling the levels, and potentially activity, of therapeutic proteins of interest. This system harbors a number of characteristics that are beneficial for conditionally regulating gene therapies including (1) minimal baseline expression (in the absence of TMP), (2) dosability,[26] (3) robust (and quick) stabilization after multiple routes of TMP administration, (4) reversibility, and (5) control of the activity of the potential gene therapy using an orally (and topically) bioavailable small-molecule drug with no/minimal side effects on vision or gene expression.

The three different regimens of TMP administration that we describe allow for simple temporal flexibility that can be adapted to suit individual project needs. TMP gavage administration yields quick (within 6 hours) and lasting stabilization of DHFR over the course of a number of days with a single administration; TMP drinking water administration can be used for daily (overnight) stabilization/destabilization regimens or long-lasting stabilization ($\geq$3 months); and TMP eye drops can be used for quick (within 6 hours) stabilization and every other day stabilization/destabilization regimens without systemic administration of the antibiotic. However, unlike systems that rely on constitutive production of a therapeutic protein of interest, a small molecule-regulated system such as the one we describe, does place the onus on researchers to determine the extent of activation (i.e., amount of TMP to use), and the ultimate regimen (i.e., when TMP should be given), which will largely depend on multiple physiological parameters related to the model system used as well as the nature of the DHFR fusion. Furthermore, looking toward the future, if such a system were applied toward the treatment of human disease, it would require patients to self-administer TMP, and therefore be subject to related patient compliance issues.

While we believe that this destabilizing DHFR system is promising for the treatment of disease, there are a number of aspects that currently limit the portability and utility of a destabilized DHFR domain to effectively control the abundance of any protein under any physiologic context and within physiologically appropriate timescales. First, in order for the destabilizing domains to be efficiently degraded in the absence of the small molecule stabilizer, the proteasome must have ready access to them. Thus, the intracellular targeting/localization of destabilizing domain fusion proteins affects their background levels and fold induction after stabilizer addition.[46] As such, historically, destabilized domains have been more successful in effectively regulating cytosolic/nuclear protein abundance rather than in the mitochondria or endoplasmic reticulum/secretory system.[46] Secondly, the physiologic context, that is, health, of the model system will likely also affect how well a destabilizing domain is turned-over in the absence of stabilizer. While our data indicate that DHFR.YFP is readily degraded in the mouse eye in the absence of TMP, we performed our experiments in healthy, young C57BL/6J mice. There is a possibility that destabilized DHFR-based system may not be effectively turned-over in certain genetic or experimental models of retinal degeneration that have compromised proteasome function,[47,48] or potentially during the course of aging.[49] Thirdly, one kinetic drawback of this DHFR-based system is that in order for stabilization of DHFR to occur, TMP must be present during the synthesis of the newly formed DHFR-fusion protein. That is to say, TMP is not able to act upon pools of unstable DHFR and subsequently quickly stabilize them. Thus, there is usually a short lag time (hours) between addition of TMP and production of adequate amounts of DHFR-based fusion protein. As physiologic cellular signaling occurs on the order of seconds to minutes,[50] use of the current destabilized DHFR-based system will require modification to achieve appropriate regulation within these shorter time frames.

The use of TMP as a small molecule stabilizer of destabilized DHFR fusion proteins in the eye is an attractive approach since it is a Food and Drug Administration-approved antibiotic with high specificity for *E. coli*. DHFR, has excellent central nervous system penetration, and has been used safely in humans for >50 years. Furthermore, TMP primarily only effects aerobic bacteria,[51,52] which comprise <1% of the total commensal human and mouse microbiome.[53,54] Yet, the potential for disruption of the gut microbiome through prolonged TMP may be a concern with long-term TMP treatments, especially with increasing evidence supporting the gut-brain communication axis[55] and the potential involvement of the gut microbiome in ocular diseases.[56,57] One potential solution to prevent gut microbiome dysbiosis would be to use TMP eye drops. Nonetheless, continued use of an antibiotic, especially a single antibiotic like TMP, can lead to the rapid development of drug-resistant bacteria,[58] and we acknowledge the need for development/application of a nonantibiotic based stabilizer system.

Another potential concern with long-term systemic TMP treatments relates to our observation of increased hemoglobin gene expression levels after 3 months of TMP treatment. It is possible that these slight, but significant changes to hemoglobin-related genes may be an indication that long-term TMP treatment can lead to alterations in folate synthesis or metabolism, potentially resulting in folate deficiency anemia (most likely through partial inhibition of mammalian DHFR), a condition that results in abnormal, subfunctional red blood cell formation. Supporting this notion, use of TMP is counter indicated in patients with folate deficiencies due to the rare possibility of anemia-related complications after high doses of TMP (and sulfamethoxazole).[59–61] Yet, these folate-related issues can likely be remedied simply by additional folate intake either through vitamins or dietary means.

In summary, we present a reliable, quick, flexible, and generalizable method for temporal and reversible control of protein abundance in the mouse retina. According to our data, prolonged TMP has no adverse effect on visual acuity, response to light, or retinal structure. Furthermore, it has only minimal effects on gene expression in the retina. An additional level of spatial control within the retina could be easily achieved by using a cell-specific promoter used to yield cell-type specific control of protein abundance. We hope that researchers will consider utilizing this DHFR-based strategy either as a tool for conditional control of protein abundance, or for gene therapy approaches that allow for spatial and temporal flexibility while minimizing potential adverse side effects due to constitutive gene expression.

Acknowledgments

The authors thank J. Cameron Millar (University of North Texas Health Science Center) for his training on intravitreal injections, Noelle Williams and Jessica Kilgore (UT Southwestern Preclinical Pharmacology Core) for their work on the quantification of TMP in mouse tissue, and Matt Petroll (UT Southwestern Department of Ophthalmology) for his assistance with fundus image quantification.

Supported by funding from the UT Southwestern Summer Medical Student Research Program (VQC). Supported through a Foundation Fighting Blindness Individual Investigator Award and receives institutional support through the Medical College of Wisconsin

NIH/NEI Visual Science Core Grant (P30 EY001931-37) and Training Grant (T32 EY014537-11) (DML). Supported by an endowment from the Roger and Dorothy Hirl Research Fund, a vision research grant from the Karl Kirchgessner Foundation, a National Eye Institute R21 Grant (EY028261), and a Career Development Award from Research to Prevent Blindness (JDH). Additional support was provided by a National Eye Institute Visual Science Core Grant (P30 EY020799) and an unrestricted grant from RPB (both to the UT Southwestern Department of Ophthalmology).

Disclosure: **S. Datta**, None; **M. Renwick**, None; **V.Q. Chau**, None; **F. Zhang**, None; **E.R. Nettesheim**, None; **D.M. Lipinski**, None; **J.D. Hulleman**, None

References

1. Acland GM, Aguirre GD, Ray J, et al. Gene therapy restores vision in a canine model of childhood blindness. *Nat Genet*. 2001;28:92–95.
2. MacLaren RE, Groppe M, Barnard AR, et al. Retinal gene therapy in patients with choroideremia: initial findings from a phase 1/2 clinical trial. *Lancet*. 2014;383:1129–1137.
3. Ghazi NG, Abboud EB, Nowilaty SR, et al. Treatment of retinitis pigmentosa due to MERTK mutations by ocular subretinal injection of adeno-associated virus gene vector: results of a phase I trial. *Hum Genet*. 2016;135:327–343.
4. Petit L, Khanna H, Punzo C. Advances in gene therapy for diseases of the eye. *Hum Gene Ther*. 2016;27:563–579.
5. Brantly ML, Chulay JD, Wang L, et al. Sustained transgene expression despite T lymphocyte responses in a clinical trial of rAAV1-AAT gene therapy. *Proc Natl Acad Sci U S A*. 2009; 106:16363–16368.
6. Toscano MG, Frecha C, Benabdellah K, et al. Hematopoietic-specific lentiviral vectors circumvent cellular toxicity due to ectopic expression of Wiskott-Aldrich syndrome protein. *Hum Gene Ther*. 2008;19:179–197.
7. Xiong W, MacColl Garfinkel AE, Li Y, Benowitz LI, Cepko CL. NRF2 promotes neuronal survival in neurodegeneration and acute nerve damage. *J Clin Invest*. 2015;125:1433–1445.
8. Jarrett SG, Boulton ME. Consequences of oxidative stress in age-related macular degeneration. *Mol Aspects Med*. 2012;33: 399–417.
9. Beatty S, Koh H, Phil M, Henson D, Boulton M. The role of oxidative stress in the pathogenesis of age-related macular degeneration. *Surv Ophthalmol*. 2000;45:115–134.
10. Zode GS, Kuehn MH, Nishimura DY, et al. Reduction of ER stress via a chemical chaperone prevents disease phenotypes in a mouse model of primary open angle glaucoma. *J Clin Invest*. 2011;121:3542–3553.
11. Griciuc A, Aron L, Ueffing M. ER stress in retinal degeneration: a target for rational therapy? *Trends Mol Med*. 2011;17:442–451.
12. Athanasiou D, Aguila M, Bellingham J, Kanuga N, Adamson P, Cheetham ME. The role of the ER stress-response protein PERK in rhodopsin retinitis pigmentosa. *Hum Mol Genet*. 2017;26:4896–4905.
13. Kroeger H, Chiang WC, Felden J, Nguyen A, Lin JH. ER stress and unfolded protein response in ocular health and disease. [published online ahead of print May 26, 2018]. *FEBS J*. doi:10.1111/febs.14522.
14. Kerrison JB, Duh EJ, Yu Y, Otteson DC, Zack DJ. A system for inducible gene expression in retinal ganglion cells. *Invest Ophthalmol Vis Sci*. 2005;46:2932–2939.
15. Chang MA, Horner JW, Conklin BR, DePinho RA, Bok D, Zack DJ. Tetracycline-inducible system for photoreceptor-specific gene expression. *Invest Ophthalmol Vis Sci*. 2000;41:4281–4287.
16. Le YZ, Zheng W, Rao PC, et al. Inducible expression of cre recombinase in the retinal pigmented epithelium. *Invest Ophthalmol Vis Sci*. 2008;49:1248–1253.
17. Herold MJ, van den Brandt J, Seibler J, Reichardt HM. Inducible and reversible gene silencing by stable integration of an shRNA-encoding lentivirus in transgenic rats. *Proc Nat Acad Sci U S A*. 2008;105:18507–18512.
18. Mansuy IM, Winder DG, Moallem TM, et al. Inducible and reversible gene expression with the rtTA system for the study of memory. *Neuron*. 1998;21:257–265.
19. Zeng H, Horie K, Madisen L, et al. An inducible and reversible mouse genetic rescue system. *PLoS Genetics*. 2008;4: e1000069.
20. Duerr J, Gruner M, Schubert SC, Haberkorn U, Bujard H, Mall MA. Use of a new-generation reverse tetracycline transactivator system for quantitative control of conditional gene expression in the murine lung. *Am J Respir Cell Mol Biol*. 2011;44:244–254.
21. Georgievska B, Jakobsson J, Persson E, Ericson C, Kirik D, Lundberg C. Regulated delivery of glial cell line-derived neurotrophic factor into rat striatum, using a tetracycline-dependent lentiviral vector. *Hum Gene Ther*. 2004;15:934–944.
22. Lamartina S, Silvi L, Roscilli G, et al. Construction of an rtTA2(s)-m2/tts(kid)-based transcription regulatory switch that displays no basal activity, good inducibility, and high responsiveness to doxycycline in mice and non-human primates. *Mol Ther*. 2003;7:271–280.
23. Chatzispyrou IA, Held NM, Mouchiroud L, Auwerx J, Houtkooper RH. Tetracycline antibiotics impair mitochondrial function and its experimental use confounds research. *Cancer Res*. 2015;75:4446–4449.
24. Moullan N, Mouchiroud L, Wang X, et al. Tetracyclines disturb mitochondrial function across eukaryotic models: a call for caution in biomedical research. *Cell Rep*. 2015;15:1681–1691.
25. Banaszynski LA, Chen LC, Maynard-Smith LA, Ooi AG, Wandless TJ. A rapid, reversible, and tunable method to regulate protein function in living cells using synthetic small molecules. *Cell*. 2006;126:995–1004.
26. Iwamoto M, Bjorklund T, Lundberg C, Kirik D, Wandless TJ. A general chemical method to regulate protein stability in the mammalian central nervous system. *Chem Biol*. 2010;17:981–988.
27. Shoulders MD, Ryno LM, Cooley CB, Kelly JW, Wiseman RL. Broadly applicable methodology for the rapid and dosable small molecule-mediated regulation of transcription factors in human cells. *J Am Chem Soc*. 2013;135:8129–8132.
28. Chen CY, Chang YL, Shih JY, et al. Thymidylate synthase and dihydrofolate reductase expression in non-small cell lung carcinoma: the association with treatment efficacy of pemetrexed. *Lung Cancer*. 2011;74:132–138.
29. Chen JJ, Genereux JC, Qu S, Hulleman JD, Shoulders MD, Wiseman RL. ATF6 activation reduces the secretion and extracellular aggregation of destabilized variants of an amyloidogenic protein. *Chem Biol*. 2014;21:1564–1574.
30. Vu KT, Zhang F, Hulleman JD. Conditional, genetically encoded, small molecule-regulated inhibition of NFkappaB signaling in RPE cells. *Invest Ophthalmol Vis Sci*. 2017;58: 4126–4137.
31. Cho U, Zimmerman SM, Chen LC, et al. Rapid and tunable control of protein stability in Caenorhabditis elegans using a small molecule. *PLoS One*. 2013;8:e72393.
32. Tai K, Quintino L, Isaksson C, Gussing F, Lundberg C. Destabilizing domains mediate reversible transgene expression in the brain. *PLoS One*. 2012;7:e46269.
33. Quintino L, Manfre G, Wettergren EE, Namislo A, Isaksson C, Lundberg C. Functional neuroprotection and efficient regu-

lation of GDNF using destabilizing domains in a rodent model of Parkinson's disease. *Mol Ther*. 2013;21:2169–2180.

34. Schweitzer BI, Dicker AP, Bertino JR. Dihydrofolate reductase as a therapeutic target. *FASEB J*. 1990;4:2441–2452.
35. Barling RW, Selkon JB. The penetration of antibiotics into cerebrospinal fluid and brain tissue. *J Antimicrob Chemother*. 1978;4:203–227.
36. Sahu B, Chavali VR, Alapati A, et al. Presence of rd8 mutation does not alter the ocular phenotype of late-onset retinal degeneration mouse model. *Mol Vis*. 2015;21:273–284.
37. Reid CA, Ertel KJ, Lipinski DM. Improvement of photoreceptor targeting via intravitreal delivery in mouse and human retina using combinatory rAAV2 capsid mutant vectors. *Invest Ophthalmol Vis Sci*. 2017;58:6429–6439.
38. Reid CA, Lipinski DM. Small and micro-scale recombinant adeno-associated virus production and purification for ocular gene therapy applications. *Methods Mol Biol*. 2018;1715:19–31.
39. Bachmanov AA, Reed DR, Beauchamp GK, Tordoff MG. Food intake, water intake, and drinking spout side preference of 28 mouse strains. *Behavior Genet*. 2002;32:435–443.
40. Prusky GT, Alam NM, Beekman S, Douglas RM. Rapid quantification of adult and developing mouse spatial vision using a virtual optomotor system. *Invest Ophthalmol Vis Sci*. 2004;45:4611–4616.
41. Sun N, Shibata B, Hess JF, FitzGerald PG. An alternative means of retaining ocular structure and improving immunoreactivity for light microscopy studies. *Mol Vis*. 2015;21:428–442.
42. Nguyen A, Hulleman JD. Evidence of alternative cystatin C signal sequence cleavage which is influenced by the A25T polymorphism. *PLoS One*. 2016;11:e0147684.
43. Nguyen A, Hulleman JD. Differential tolerance of "pseudopathogenic" tryptophan residues in calcium-binding EGF domains of short fibulin proteins. *Exp Eye Res*. 2015;130:66–72.
44. Remtulla S, Hallett PE. A schematic eye for the mouse, and comparisons with the rat. *Vis Res*. 1985;25:21–31.
45. Koury MJ, Ponka P. New insights into erythropoiesis: the roles of folate, vitamin B12, and iron. *Annu Rev Nutr*. 2004;24:105–131.
46. Sellmyer MA, Chen LC, Egeler EL, Rakhit R, Wandless TJ. Intracellular context affects levels of a chemically dependent destabilizing domain. *PLoS One*. 2012;7:e43297.
47. Lobanova ES, Finkelstein S, Skiba NP, Arshavsky VY. Proteasome overload is a common stress factor in multiple forms of inherited retinal degeneration. *Proc Nat Acad Sci U S A*. 2013;110:9986–9991.
48. Lobanova ES, Finkelstein S, Li J, et al. Increased proteasomal activity supports photoreceptor survival in inherited retinal degeneration. *Nature Comm*. 2018;9:1738.
49. Low P. The role of ubiquitin-proteasome system in ageing. *Gen Comp Endocrinol*. 2011;172:39–43.
50. Kholodenko BN. Cell-signalling dynamics in time and space. *Nat Rev*. 2006;7:165–176.
51. Rosenblatt JE, Stewart PR. Lack of activity of sulfamethoxazole and trimethoprim against anaerobic bacteria. *Antimicrob Agents Chemother*. 1974;6:93–97.
52. Then RL, Angehrn P. Low trimethoprim susceptibility of anaerobic bacteria due to insensitive dihydrofolate reductases. *Antimicrob Agents Chemother*. 1979;15:1–6.
53. Harris MA, Reddy CA, Carter GR. Anaerobic bacteria from the large intestine of mice. *Appl Environ Microbiol*. 1976;31:907–912.
54. Maier E, Anderson RC, Roy NC. Understanding how commensal obligate anaerobic bacteria regulate immune functions in the large intestine. *Nutrients*. 2014;7:45–73.
55. Carabotti M, Scirocco A, Maselli MA, Severi C. The gut-brain axis: interactions between enteric microbiota, central and enteric nervous systems. *Ann Gastroenterol*. 2015;28:203–209.
56. Horai R, Zarate-Blades CR, Dillenburg-Pilla P, et al. Microbiota-dependent activation of an autoreactive T cell receptor provokes autoimmunity in an immunologically privileged site. *Immunity*. 2015;43:343–353.
57. Rowan S, Jiang S, Korem T, et al. Involvement of a gut-retina axis in protection against dietary glycemia-induced age-related macular degeneration. *Proc Nat Acad Sci U S A*. 2017;114:E4472–E4481.
58. Toprak E, Veres A, Michel JB, Chait R, Hartl DL, Kishony R. Evolutionary paths to antibiotic resistance under dynamically sustained drug selection. *Nat Genet*. 2011;44:101–105.
59. Kobrinsky NL, Ramsay NK. Acute megaloblastic anemia induced by high-dose trimethoprim-sulfamethoxazole. *Ann Intern Med*. 1981;94:780–781.
60. Frieder J, Mouabbi JA, Zein R, Hadid T. Autoimmune hemolytic anemia associated with trimethoprim-sulfamethoxazole use. *Am J Health Syst Pharm*. 2017;74:894–897.
61. Williams MF, Doss EP, Montgomery M. Possible trimethoprim-sulfamethoxazole-induced hemolytic anemia: a case report. *J Pharm Pract*. 2017;30:653–657.

Investigative Ophthalmology & Visual Science